ACCOUNTS of chemical research

Article

pubs.acs.org/accounts

Optimizing Calculations of Electronic Excitations and Relative Hyperpolarizabilities of Electrooptic Chromophores

Lewis E. Johnson, Larry R. Dalton, and Bruce H. Robinson*

Department of Chemistry, University of Washington, Seattle, Washington 98195-1700, United States

CONSPECTUS: Organic glasses containing chromophores with large first hyperpolarizabilities (β) are promising for compact, high-bandwidth, and energy-efficient electro-optic devices. Systematic optimization of device performance requires development of materials with high acentric order and enhanced hyperpolarizability at operating wavelengths. One essential component of the design process is the accurate calculation of optical transition frequencies and hyperpolarizability. These properties can be computed with a wide range of electronic structure methods implemented within commercial and open-source software packages. A wide variety of methods, especially hybrid density-functional theory (DFT) variants have been used for this purpose. However, in order to provide predictions useful to chromophore designers, a method must be able to consistently predict the relative ordering of standard and novel materials. Moreover, it is important to distinguish between the resonant and nonresonant contribution to the hyperpolarizabiliy and be able to estimate the trade-off between improved β and unwanted absorbance (optical loss) at the target device's operating wavelength.

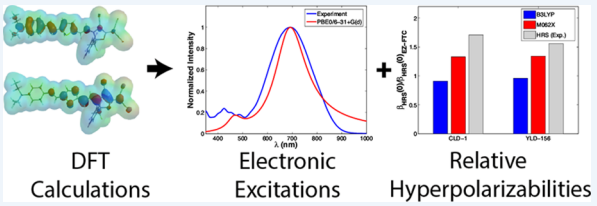

Therefore, we have surveyed a large variety of common methods for computing the properties of modern high-performance chromophores and compared these results with prior experimental hyper-Rayleigh scattering (HRS) and absorbance data. We focused on hybrid DFT methods, supplemented by more computationally intensive Møller−Plesset (MP2) calculations, to determine the relative accuracy of these methods. Our work compares computed hyperpolarizabilities in chloroform relative to standard chromophore EZ-FTC against HRS data versus the same reference.

We categorized DFT methods used by the amount of Hartree−Fock (HF) exchange energy incorporated into each functional. Our results suggest that the relationship between percentage of long-range HF exchange and both β_{HRS} and λ_{max} is nearly linear, decreasing as the fraction of long-range HF exchange increases. Mild hybrid DFT methods are satisfactory for prediction of λ_{max}. However, mild hybrid methods provided qualitatively incorrect predictions of the relative hyperpolarizabilities of three high-performance chromophores. DFT methods with approximately 50% HF exchange, and especially the Truhlar M062X functional, provide superior predictions of relative β_{HRS} values but poorer predictions of λ_{max}. The observed trends for these functionals, as well as range-separated hybrids, are similar to MP2, though predicting smaller absolute magnitudes for β_{HRS}.

Frequency dependence for β_{HRS} can be calculated using time-dependent DFT and HF methods. However, calculation quality is sensitive not only to a method's ability to predict static hyperpolarizability but also to its prediction of optical resonances. Due to the apparent trade-off in accuracy of prediction of these two properties and the need to use static finite-field methods for MP2 and higher-level hyperpolarizability calculations in most codes, we suggest that composite methods could greatly improve the accuracy of calculations of β and λ_{max}.

INTRODUCTION

Systematic improvement of electro-optic performance through theory-aided design requires accurate calculation of both linear and nonlinear optical properties of candidate chromophores.[1−3] Such calculations are important for presynthesis screening,[4] to provide insight on whether a difficult synthesis may be worth pursuing, and for assisting in deconvoluting the effects of molecular nonlinearity (as quantified by the first hyperpolarizability, β) versus ordering in contributing to the electro-optic (EO) behavior of a material.[5] Performance of an EO material is typically quantified by the electro-optic coefficient[1]

$$r_{33} = \frac{-2\chi^{(2)}_{zzz}}{{n_\omega}^4} = \frac{-2g(\omega, \varepsilon)\rho_N\beta_{zzz}(-\omega, 0, \omega)\langle\cos^3\theta\rangle}{{n_\omega}^4} \quad (1)$$

where $g(\omega,\varepsilon)$ is the product of frequency and dielectric-dependent local field factors, ρ_N is the number density of the chromophores, $\beta_{zzz}(-\omega,0,\omega)$ is the component of the molecular first hyperpolarizability along the dipole moment (defined as the z-axis in the frame of the molecule) for interacting low-frequency and optical fields, and $\langle\cos^3\theta\rangle$ is the bulk acentric order parameter. Development of improved EO materials requires optimization of both the molecular hyperpolarizability and the bulk acentric order,[6] and the wide variation in order parameters[2] requires measurement or simulation of the hyperpolarizabilities of chromophores in isolation. Accurate simulations are

Special Issue: DFT Elucidation of Materials Properties

Received: February 20, 2014
Published: June 26, 2014

   dx.doi.org/10.1021/ar5000727 | Acc. Chem. Res. 2014, 47, 3258−3265

particularly crucial because the Pockels effect hyperpolarizability $\beta_{zzz}(-\omega,0,\omega)$ cannot be directly measured.

Second-harmonic hyperpolarizability $\beta(-2\omega,\omega,\omega)$ can be measured in solution using hyper-Rayleigh scattering[7] (HRS) or electric-field induced second harmonic generation[8] (EFISHG). Because the latter technique requires accurate measurements of dipole moments to extract β from measurements, we will focus our comparison on HRS data.

HRS, developed by Clays et al.,[7] measures the intensity of incoherent emission of frequency-doubled light

$$I_{2\omega} \propto \sum_i \rho_{N,i}{\beta_{\mathrm{HRS},i}}^2(-2\omega, \omega, \omega){I_0}^2(\omega) \tag{2}$$

in response to an intense laser pulse of intensity I_0; the constant of proportionality depends on the experimental geometry and dielectric environment (local field factors). The constant of proportionality can be eliminated by measuring the signal relative to a standard material. Because HRS measurements are conducted in isotropic media, they measure a rotationally averaged hyperpolarizability β_{HRS}.[9,10] In the case of a linear charge transfer chromophore, the HRS average is approximately related to the tensor component along the dipole axis as

$$\beta_{\mathrm{HRS}}(-2\omega, \omega, \omega) \approx \sqrt{\frac{6}{35}}\beta_{zzz}(-2\omega, \omega, \omega) \tag{3}$$

Because the Pockels and second-harmonic hyperpolarizities have different frequency dependence, the frequency dispersion must still be adjusted using the two-level model[5,8]

$$\beta(-2\omega, \omega, \omega) \approx \left|\frac{{\omega_{\max}}^4}{(\omega^2 - {\omega_{\max}}^2)(\omega^2 - 4{\omega_{\max}}^2)}\right|\beta(0)$$
$$\beta(-\omega, 0, \omega) \approx \frac{3{\omega_{\max}}^2 - \omega^2}{3({\omega_{\max}}^2 - \omega^2)^2}\beta(0) \tag{4}$$

where ω is the frequency of the light field and $\omega_{\max}$ is the frequency of the lowest charge-transfer excitation of the chromophore. However, the two-level model is an incomplete description of the frequency dependence of hyperpolarizability due to contributions from other electronic states.[1,11]

In contrast with experimental techniques such as HRS, calculations using coupled-perturbed Hartree−Fock[12,13] (CPHF), real-time time-dependent density functional theory,[14] (RT-TDDFT), sum-over-states[15] (SOS), or coupled-cluster response theory[16,17] can directly obtain the entire hyperpolarizability tensor for applied fields of arbitrary frequency within arbitrary dielectric environments. Static hyperpolarizabilities can also be obtained using finite-field (FF) techniques in combination with many different electronic structure methods.[3] Previous computational studies have provided significant insight into general trends in chromophore hyperpolarizabilities,[3,15] relative hyperpolarizabilities of common chromophores versus experimental standards,[18] frequency dispersion of high-performance chromophores,[14] hyperpolarizabilities of small solvent molecules,[19,20] and solvent dependence of hyperpolarizability,[11,21] as well as hyperpolarizability ratios in nonlinear optical switches.[22] However, quantitative comparison of calculated absolute hyperpolarizabilities remains difficult due to the variety of approximations and calibration standards used in the literature.[23]

One significant challenge is reliably and efficiently predicting the relative hyperpolarizabilities of modern, high-performance chromophores. These often have molecular weights on the order of 600−1200 amu. For reasons of computational efficiency, routine electronic structure calculations on chromophores of this size are typically conducted using density-functional theory[2,24,25] (DFT) or semiempirical Hartree−Fock (HF) based methods such as INDO[15,26] due to their favorable scaling with number of basis functions. Higher-order methods such as coupled-cluster theory have been used for reference calculations on a variety of systems such as *p*-nitroaniline[19] and other prototypical push−pull systems.[27] Second-order Møller−Plesset perturbation theory (MP2) has been reported to give reasonable estimates of hyperpolarizabilities at lower costs than coupled-cluster theory,[28] typically recovering most of the correlation energy in calculations on small molecules.[10] MP2 and methods of similar computational intensity such as CC2[29] are now tractable on modest hardware but consume far more computing resources than DFT, limiting utility for routine screening of large numbers of chromophores. Both DFT and semiempirical methods are parametrization-dependent, and some DFT methods such as the commonly used B3LYP[30,31] functional are insensitive to changes in chromophore structure that produce large differences in experimentally determined hyperpolarizability and EO activity. While a wide variety of electronic structure methods can be used to predict large-scale trends in hyperpolarizability,[3] predicting differences between chromophores of similar structure requires careful selection of a calculation method and metric for comparison.

A related issue is the prediction of excitation energies, which are critical for both understanding frequency dispersion of hyperpolarizability[5] and optical loss in device applications.[32] As with hyperpolarizabilities, excitation energies can be evaluated using a wide variety of methods,[33,34] ranging from configuration interaction singles (CIS) and TD-HF/TD-DFT to correlated methods such as CIS(D), CC2, and EOM-CCSD. For larger organic chromophores, TD-DFT using common hybrid functionals such as PBE0[35] and B3LYP often performs very well.[32,36] However, for a method to be suitable for predicting frequency-dependent hyperpolarizabilities, it must provide a reasonable prediction not only of electronic excitations but also of the static hyperpolarizability.

Finally, calculation methods used in surveying chromophore hyperpolarizabilities would optimally have minimal dependence on empirical parametrization. Many of the DFT methods currently in use for molecular systems are so-called hybrid functionals,[31,37,38] which replace a portion of the local spin density (LSDA) or generalized-gradient approximation (GGA) exchange energy with nonlocal Hartree−Fock (HF) exchange. This is done in order to cancel out the tendency for DFT to be insensitive to longer-range interaction between orbitals due to self-interaction error,[33,39] while partially correcting for Hartree−Fock's neglect of electron correlation through incorporation of LSDA/GGA correlation. In common formulations such as B3LYP and PBE0 (mild hybrids), the amount of Hartree−Fock exchange used is on the order of 25% or less. While this partially mitigates errors in (de)localization of electron density, mild hybrid functionals still provide an incorrect estimate of long-range Coulomb interactions and have difficulty in predicting energies of charge-transfer states,[39] including sometimes predicting spurious low-lying states.[39−41] Hybrids with larger quantities of HF exchange improve screening[42] of electron density over long distances and reduces spurious charge

separation in long conjugated systems.[43] However, increasing the fraction of HF exchange significantly blue shifts electronic excitations.[40] Range-separated functionals such as LC-BLYP[44] and CAM-B3LYP,[45] in which the amount of HF exchange smoothly varies from a small value at short distance to a larger value at long distance, have resulted in improved treatment of charge transfer states,[33,45] and properties of polymethineimine chains.[46] These methods blue shift absolute excitation energies in a similar manner to high-HF functionals. These functionals also introduce one or more additional parameters controlling the transition between local and HF exchange; optimization of these parameters is currently an active field of research.[47−49] Other methods have been used to mitigate the overlocalization in typical DFT methods, such as invocation of higher derivatives of the local density[50,51] (meta-GGA), adding MP2 correlation to the functional,[52] or extensive empirical parametrization (dozens of adjustable parameters), as used in the Minnesota functionals developed by the Truhlar group.[53,54]

MODEL SYSTEM

A particularly striking example of the difficulty of accurately predicting β_{HRS} can be seen from the set of high-performance chromophores examined[11] by Bale et al.; the YLD-156 and CLD-1 chromophores were determined by HRS to exhibit nearly twice the hyperpolarizability of reference chromophore EZ-FTC. Calculations at the B3LYP/6-31G(d) level, while sensitive to the solvent dielectric environment, were insensitive to structural differences. The structures of the three chromophores are shown in Figure 1.

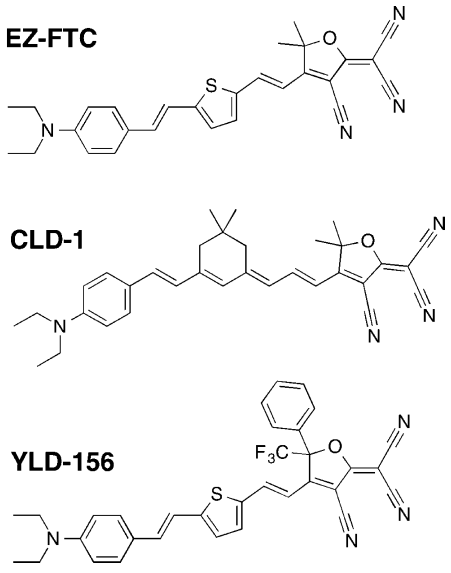

Figure 1. Two-dimensional structures of the chromophores discussed in this Account. Alkyl chains on the donor have been truncated to ethyl groups for computational efficiency.

The following work evaluates the performance of eight hybrid functionals for predicting hyperpolarizability and charge-transfer excitations. Three wave function-based methods, Hartree−Fock, the computationally inexpensive semiempirical PM6 method, combined with electronic excitations calculated with the ZINDO[55,56] semiempirical method, and the more accurate but expensive MP2 method, were used for comparison. Methods used are shown in Table 1, along with the fraction of Hartree−Fock exchange energy used in the functional at asymptotically long and short distances.

Table 1. Methods Used for Comparison of Hyperpolarizabilities and Excitation Energies, Showing Amounts of Short-Range (SR) and Long-Range (LR) Hartree−Fock Exchange

		% HF exchange		
method	type	SR	LR	range-separation parameter (ω), au^{-1}
B3LYP[30,31]	hybrid GGA	20	20	*a*
PBE0[35] (pbe1pbe)	hybrid GGA	25	25	*a*
BHandHLYP[57]	hybrid GGA	50	50	*a*
M062X[58]	hybrid meta-GGA	54	54	*a*
CAM-B3LYP[45]	range-separated GGA	19	65	0.33
LC-BLYP[44]	range-separated GGA	0	100	0.47
ωB97X[59]	range-separated GGA	15.8	100	0.30
M11[60]	range-separated meta-GGA	43	100	0.25
Hartree−Fock	*ab initio* wave function	100	100	*a*
PM6[61]	semiempirical HF	100	100	*a*
ZINDO[55]	semiempirical HF	100	100	*a*
MP2	post-HF wave function	100	100	*a*

[a]Not applicable.

Experimental excitation wavelengths and hyperpolarizability ratios relative to EZ-FTC are shown in Table 2, along with the two-level model resonance enhancement factor (TLF) for each chromophore. Hyperpolarizabilities are reported as ratios; HRS measurements are typically conducted relative to a standard chromophore,[6,18] such as EZ-FTC in this case[11] or pure solvent.[7]

Table 2. Experimental Reference Data Used As Benchmarks for Calculations[a]

chromophore	EZ-FTC	CLD-1	YLD-156
λ_{max} (nm)	676	691	753
TLF	2.30	2.42	3.15
Rel. β_{HRS} (1907 nm)	1 (ref)	1.80 ± 0.08	2.14 ± 0.25
Rel. β_{HRS} (0)	1 (ref)	1.71 ± 0.08	1.56 ± 0.18

[a]All data were collected in chloroform and are from Bale et al.,[11] except for the excitation wavelength of EZ-FTC, which is from Firestone.[62]

Functionals were compared using three metrics: relative static hyperpolarizability, relative HRS hyperpolarizabilities at 1906 nm, and dominant (lowest charge transfer) excitation energies. Static experimental hyperpolarizabilities were extrapolated with the two-level model (eq 4). Relative hyperpolarizabilities (ratio of the performance of a test chromophore versus a standard) were chosen as a metric in order to more directly compare with HRS measurements and based on the work of Suponitsky, Liao, and Masunov, which found that a selection of four DFT techniques had greater success at predicting relative values than absolute magnitudes.[18] The correlation between hyperpolarizability and excitation energies versus the amount of Hartree−

dx.doi.org/10.1021/ar5000727 | Acc. Chem. Res. 2014, 47, 3258−3265

Fock exchange in each functional was also explored. Because the three chromophores examined in this Account are particularly sensitive to calculation method, observed trends should be useful for a wide variety of push−pull chromophores.

ELECTRONIC STRUCTURE CALCULATIONS

All calculations were performed with commercially available versions of Gaussian 09[63] and used the 6-31+G(d) basis set, which had previously been determined to provide reasonable performance at low cost for larger ONLO chromophores.[21] All calculations were run in PCM chloroform. Calculations on PM6 geometries used the ZINDO method for electronic excitations due to its high accuracy in this application.[56]

Hyperpolarizabilities were calculated by differentiation of total electronic energy E with respect to an applied electric field F. By the Hellman−Feynman theorem, the dipole moment, polarizability, and hyperpolarizabilities can be calculated by treating the applied field as a weak perturbation to the Hamiltonian, such that[12,64]

$$E(F) = E_0 + \frac{\partial E}{\partial F_i}F_i + \frac{1}{2}\frac{\partial^2 E}{\partial F_i F_j}F_i F_j + \frac{1}{6}\frac{\partial^3 E}{\partial F_i F_j F_k}F_i F_j F_k \ldots \quad (5)$$

which is equivalent to

$$E(F) = E_0 - \mu_i F_i - \alpha_{ij}F_i F_j - \beta_{ijk}F_i F_j F_k \ldots \quad (6)$$

These derivatives can be calculated with respect to either a static or time-varying field and can be calculated numerically or analytically.[2,12] Single-determinant calculations used in this work used CP-TDHF/CP-TDDFT analytic differentiation.[12] MP2 calculations used numerical differentiation of analytic dipole moments versus a finite field of ±0.001 au, which has previously been found to be adequate for medium-sized chromophores.[3] Hyperpolarizabilities were scaled to use the perturbation series convention as shown in eq 6.

COMPARISON OF METHODS

Electronic Excitations

Absolute excitation energies were strongly method-dependent. The mild hybrids (especially PBE0) were particularly accurate, consistent with prior calculations on TCF-based chromophores,[32] as well as a variety of other small organic dyes[36] and conjugated polymers.[65] Use of large fractions of HF exchange resulted in an overestimate of the excitation energies, consistent with the results of Dreuw and co-workers.[42] Range-separated functionals significantly overestimated excitation energies, with LC-BLYP, ωB97X, and M11 generating errors on the order of those from TDHF, which are typically large.[33] This likely indicates that the charge transfer distance is sufficiently long that the short-range portion of the exchange functional plays a relatively small role compared with the long-range (pure HF) portion. This is consistent with results by Brédas and co-workers examining optimal range-separation parameters for different conjugation lengths.[66] Excitation energies were also compared with the amount of long-range Hartree−Fock exchange in the hybrid DFT methods used; results appear in Figure 2.

Excitation energies of all three chromophores were strongly and linearly correlated ($R^2 > 0.93$, $p < 0.01$) with long-range HF exchange, consistent with results by Brédas and co-workers.[49] We did not observe a corresponding correlation for short-range HF exchange. The ordering of excitation wavelengths remained consistent between methods. Given that dependence on the amount of HF exchange is far greater than the difference in excitation energies between the chromophores, it is important that calculations within a test set of molecules be compared only with those calculated by the same method and that absolute values of the excitation energies be treated with caution.

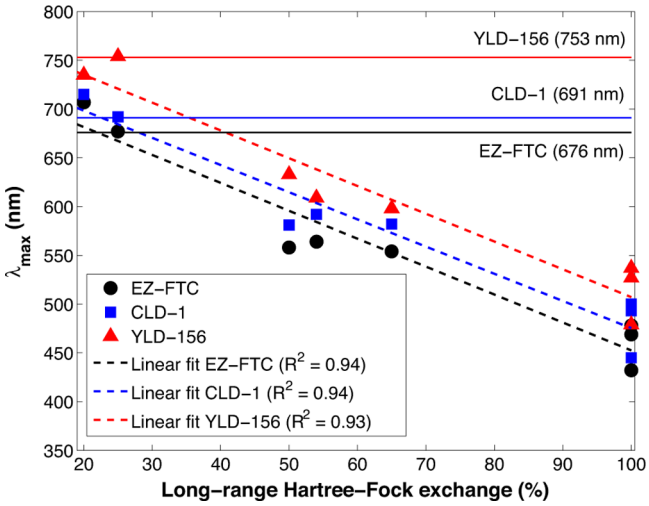

Figure 2. First charge-transfer excitation energy of EZ-FTC and CLD-1 in chloroform as a function of long-range Hartree−Fock exchange in hybrid DFT methods.

Hyperpolarizability

The relative hyperpolarizabilities of CLD-1 and YLD-156 compared with EZFTC were calculated in the static limit (see Table 3) and at 1906 nm. Experimental HRS results used for comparison were extrapolated to the static limit using the two-level model (eq 4).

Table 3. Static Hyperpolarizability Ratios ($\beta_{HRS}(0)$) versus EZ-FTC

method	EZ-FTC (10^{-30} esu)	CLD-1/EZ-FTC	YLD-156/EZ-FTC
B3LYP	630	0.91	0.96
PBE0	569	1.02	1.07
BHandHLYP	362	1.23	1.30
M062X	389	1.33	1.34
CAM-B3LYP	357	1.32	1.35
LC-BLYP	135	1.30	1.41
ωB97X	181	1.41	1.44
M11	203	1.36	1.41
HF	79	1.22	1.42
PM6	143	1.05	1.29
MP2//B3LYP	751	1.51	1.42
MP2//M062X	428	1.39	1.50
experiment (TLM)	*a*	*1.71 ± 0.08*	*1.56 ± 0.18*

[a]Not applicable.

Rotationally averaged hyperpolarizabilities $\beta_{HRS}(-2\omega,\omega,\omega)$ are shown in Figure 3 at 1906 nm; the dotted red bands indicate the range of experimental uncertainty in the ratio.

Here, the two mild hybrids indicate little difference in hyperpolarizability among the three chromophores, as previously reported both in chloroform[11] and *in vacuo*.[3] B3LYP incorrectly predicts higher performance for EZ-FTC than for CLD-1. Range-separated functionals perform well, especially ωB97X. M062X also performs well, consistent with the results of Castet

dx.doi.org/10.1021/ar5000727 | Acc. Chem. Res. 2014, 47, 3258−3265

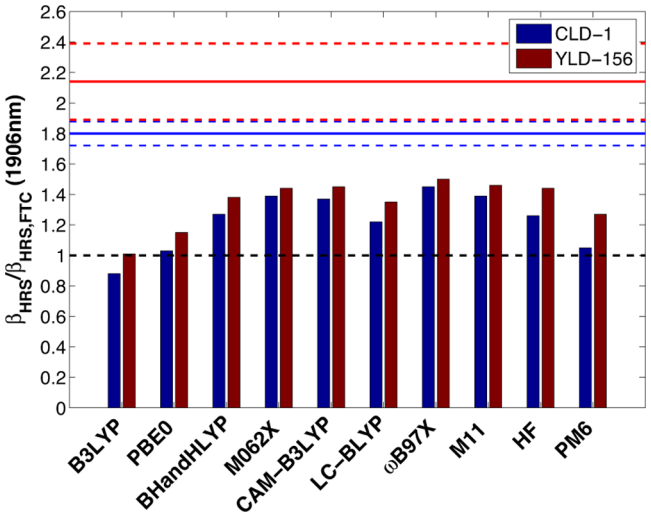

Figure 3. Comparison of hyperpolarizability ratios versus EZ-FTC at 1906 nm in chloroform. Experimental ratios and their standard deviations are shown with solid and dashed lines, respectively.

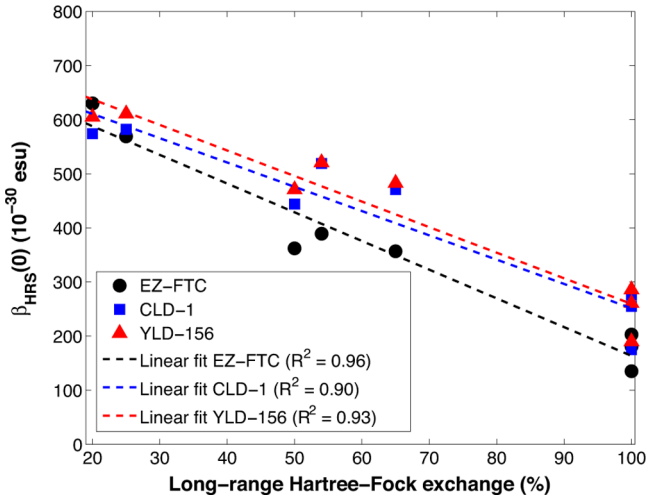

Figure 4. $\beta_{HRS}(0)$ of EZ-FTC and CLD-1 in chloroform as a function of long-range Hartree–Fock exchange in hybrid DFT methods.

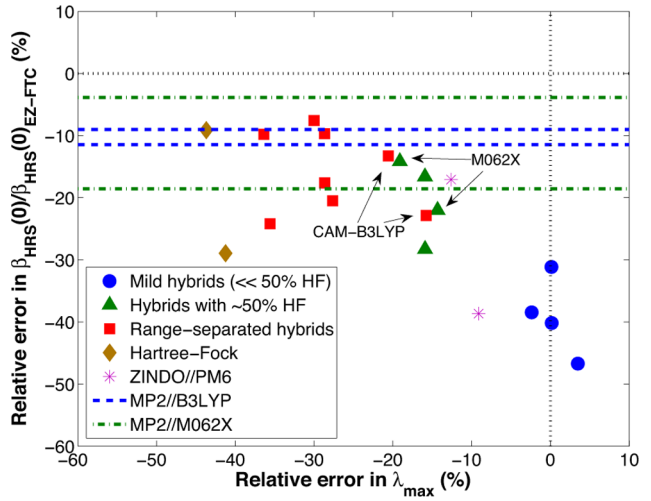

Figure 5. Comparison of errors in the $\beta_{HRS}(0)$ ratios versus EZ-FTC versus errors in the lowest charge-transfer excitation energy of CLD-1 and YLD-156. DFT methods are divided into three families. Wave function-based methods are shown for comparison; MP2 methods are represented as lines due to the absence of an excitation calculation. Each point or line represents a single calculation on one chromophore.

et al.[22] and work by Liao and co-workers[18] using the earlier M052X functional.[53] The MP2 method using the B3LYP geometry was closest to experiment and consistent with MP2's relative accuracy compared with higher-order wave function-based methods[28,43,67] such as MP4. While limited literature is available on calculation of hyperpolarizability using range-separated functionals, CAM-B3LYP was found to perform well for predicting hyperpolarizabilities of polyacetylenes,[68] as well as of exotic annulenes.[69] In the latter case, the M052X and BHandHLYP functionals also performed well. Range-separated functionals were also found to closely track MP2 calculations for substituted (*E*)-benzaldehyde phenylhydrazones.[70] Calculations for CLD-1 were on average closer to experiment than those for YLD-156, reversing the trend seen in the static calculations (Table 3); this is due to the substantially redder absorption maximum of YLD-156, and correspondingly larger influence of resonance enhancement at 1906 nm.

The relationship between β_{HRS} and the amount of Hartree–Fock exchange used in the DFT functionals was also analyzed in a similar manner to that used for the dipole moment and excitation energies. Calculated static hyperpolarizabilities for each chromophore are shown in Figure 4. Once again, a strong linear trend ($R^2 > 0.9$, $p < 0.01$) is observed.

DFT results were also compared with several wave function-based methods (see Table 3). HF and PM6 are qualitatively similar to high-HF DFT methods, but with much lower magnitude of the hyperpolarizability. MP2//M062X performs similarly to M062X, and MP2//B3LYP provides the most accurate relative values, with larger magnitudes closer to those observed based on HRS and EO activity.[11]

OVERALL ACCURACY

Relative errors in the static hyperpolarizability ratio and in the excitation energies of the chromophores were compared by calculation type in order to determine the feasibility of using a single method for both excitation and hyperpolarizability calculations. Results are shown in Figure 5.

Errors in the absolute excitation energy and relative hyperpolarizability trended in opposite directions because the amount of Hartree–Fock exchange is varied; mild hybrids such as B3LYP predict excitation energies well at the expense of predicting relative hyperpolarizabilities, and range-separated hybrids predict the hyperpolarizability ratio well at the expense of quantitative excitation energies. Hybrids with nearly 50% HF exchange gave intermediate results. Hartree–Fock itself did not perform well for either metric, and PM6 severely underestimated the hyperpolarizability ratio for CLD-1 but performed better for YLD-156. Static hyperpolarizability calculations for most methods were superior for YLD-156 (consistent with Bale et al.[11]) compared with CLD-1, though dynamic hyperpolarizability calculations were worse (see Figure 3). Accuracy was further quantified using the length of the two-dimensional error vector as a figure of merit

dx.doi.org/10.1021/ar5000727 | *Acc. Chem. Res.* 2014, 47, 3258–3265

$$\mathrm{FOM} = \left(\frac{1}{N_\beta} \sum_{i=1}^{N_\beta} \left(\frac{\beta_{\mathrm{HRS}} - \beta_{\mathrm{HRS}}(\mathrm{exp})}{\beta_{\mathrm{HRS}}(\mathrm{exp})} \right)^2 + \frac{1}{N_\lambda} \sum_{j=1}^{N_\lambda} \left(\frac{\lambda_{\max} - \lambda_{\max}(\mathrm{exp})}{\lambda_{\max}(\mathrm{exp})} \right)^2 \right)^{1/2} \quad (7)$$

to provide an estimate of the total deviation from experiment. Accuracies using this metric and its components are tabulated in Table 4.

Table 4. Accuracy Ranking of DFT, HF, and MP2 Methods

method	$\lambda_{\max}$ rank	$\beta_{\mathrm{HRS}}(0)$ rank	FOM	FOM rank
B3LYP	2	12	0.468	9
PBE0	**1**	11	0.402	7
BHandHLYP	4	8	0.324	3
M062X	5	6	**0.262**	**1**
CAM-B3LYP	6	7	0.278	2
LC-BLYP	9	5	0.430	8
ωB97X	7	3	0.336	5
M11	8	4	0.327	6
HF	10	8	0.504	10
ZINDO//PM6	3	10	0.397	4
MP2//B3LYP	*a*	**1**	*a*	*a*
MP2//M062X	*a*	2	*a*	*a*

[a]Not applicable.

Despite not being the best performer for either property alone, the M062X functional minimizes the combined error, with the CAM-B3LYP functional being a close second. While the MP2 methods performed very well for hyperpolarizability, they did not receive an overall rank due to difficulties in performing CIS(D) calculations in solvent but should still be considered for calculating ground-state properties. The ωB97X functional performed very well for hyperpolarizabilities (nearly on par with MP2) but not for excitations. B3LYP and HF ranked poorly due to large errors in either $\lambda_{\max}$ (HF) or relative hyperpolarizability (B3LYP). The poor performance of HF for $\lambda_{\max}$ is worrisome for its use in resonance corrections[10,18] for finite field calculations at near-resonant wavelengths.

Based on these aggregate results, we recommend M062X and CAM-B3LYP for routine calculations of off-resonance relative hyperpolarizabilites of midsize chromophores. We do not recommend Hartree−Fock or B3LYP; the latter produced qualitatively inaccurate predictions of the ordering of the three chromophores. We recommend PBE0 for electronic spectra calculations on organic chromophores with the caveat that it may not provide reliable information on hyperpolarizabilties.

CONCLUSION AND OUTLOOK

Based on both static and frequency-dependent calculations on three high performance electro-optic chromophores, mild hybrid functionals (<50% Hartree−Fock exchange) are inadequate for reliably predicting trends in the relative hyperpolarizabilities of chromophores with long bridges and strong acceptors (such as TCF variants). Functionals with more than 50% Hartree−Fock exchange, as well as those incorporating distance-dependent Hartree−Fock exchange, exhibit superior performance for hyperpolarizabilities at the expense of severely blue-shifted excitation energies. However, the PBE0 functional performs well for electronic excitation energies. The trade-off between accuracy in calculating hyperpolarizabilities and excitation energies complicates the calculation of the resonant contribution to the hyperpolarizability, and the linear dependence of absolute hyperpolarizability on Hartree−Fock exchange greatly complicates predicting the absolute performance of chromophores based on DFT calculations.

Because relative hyperpolarizabilities are much less sensitive to the fraction of HF exchange above a certain threshold (∼50%), they represent a more accessible metric for DFT calculations. Estimates of absolute hyperpolarizabilities could then be obtained by multiplying these ratios by experimental values or results from high-level calculations on standard chromophores (PNA, Disperse Red 1, EZ-FTC, etc.). Calculations at the MP2 level may be adequate for this purpose, but higher-level calculations (e.g., CCSD or CC2) are recommended if possible.

None of the DFT methods examined provide an ideal combination of low error in hyperpolarizability and in electronic excitations, although M062X and CAM-B3LYP come closest. Possible routes for improvement include tuning a range-separated functional such as CAM-B3LYP specifically for calculations on organic EO chromophores, as Autschbach and co-workers have done for circular dichroism spectra,[48] or using a composite method (e.g., using B3LYP for geometry, CAM-B3LYP for hyperpolarizability, and PBE0 for frequency dependence). Alternately, faster, approximate MP2 methods could be used to enable routine high-level calculations.

However, despite imperfect accuracy, modern functionals such as M062X and CAM-B3LYP provide reasonable approximation of the trends in hyperpolarizability and can provide insight on trends in chromophore properties relevant to theory-aided design. Further critical analysis of calculation methods would require calibration against a larger set of chromophores than the three explored here and highly accurate HRS data on the reference chromophores or very high-level (e.g., CCSD) calculations for verification.

AUTHOR INFORMATION

Corresponding Author

*E-mail: robinson@chem.washington.edu.

Notes

The authors declare no competing financial interest.

Biographies

Lewis E. Johnson received his B.A. from Pomona College in 2007 and his Ph.D. from the University of Washington in 2012 working with B. H. Robinson. He is currently a Research Associate at UW after teaching at Pomona College in 2013−2014.

Larry R. Dalton received his B.S. (1965) and M.S. (1966) from the Honors College of Michigan State University with James Dye and A.M. and Ph.D. (1971) from Harvard with Alvin Kwiram. He is the Rabinovitch Chair Professor Emeritus at the University of Washington. He is a Fellow of the ACS, MRS, OSA, SPIE, and AAAS and a Senior Member of IEEE. ACS-related awards include the Award in the Chemistry of Materials and the Tolman and Pauling Medals. IEEE/LEOS awards include the William Streifer Award for Scientific Achievement.

Bruce H. Robinson received his A.B. from Princeton in 1967 and Ph.D. from Vanderbilt in 1975 with L. J. Schaad and L. R. Dalton. He joined the faculty at the University of Washington in 1980 and is currently the Dalton Professor of Chemistry at UW.

■ ACKNOWLEDGMENTS

This Account is substantially derived from Chapter 5 of L.E.J.'s dissertation,[71] "Multi-Scale Modeling of Organic Electro-Optic Materials." The authors thank Xiaosong Li, Bruce E. Eichinger, Christine M. Isborn, Koen Clays, and members of the Robinson, Dalton, and Li groups for useful discussion. The authors acknowledge partial financial support for this work from the National Science Foundation (Grants STC-MDITR DMR-0120967, DMR-1303080, and DMR-0905686), the Air Force Office of Scientific Research (Grant FA9550-09-1-0589), and the University of Washington Student Technology Fund.

■ REFERENCES

(1) Dalton, L. R.; Sullivan, P. A.; Bale, D. H. Electric Field Poled Organic Electro-optic Materials: State of the Art and Future Prospects. *Chem. Rev.* **2010**, *110*, 25−55.

(2) Dalton, L. R.; Benight, S. J.; Johnson, L. E.; Knorr, D. B.; Kosilkin, I.; Eichinger, B. E.; Robinson, B. H.; Jen, A. K. Y.; Overney, R. M. Systematic Nanoengineering of Soft Matter Organic Electro-optic Materials. *Chem. Mater.* **2011**, *23*, 430−445.

(3) Isborn, C. M.; Leclercq, A.; Vila, F. D.; Dalton, L. R.; Brédas, J. L.; Eichinger, B. E.; Robinson, B. H. Comparison of Static First Hyperpolarizabilities Calculated with Various Quantum Mechanical Methods. *J. Phys. Chem. A* **2007**, *111*, 1319−1327.

(4) Sullivan, P. A.; Dalton, L. R. Theory-Inspired Development of Organic Electro-optic Materials. *Acc. Chem. Res.* **2009**, *43*, 10−18.

(5) Sullivan, P. A.; Rommel, H. L.; Takimoto, Y.; Hammond, S. R.; Bale, D. H.; Olbricht, B. C.; Liao, Y.; Rehr, J.; Eichinger, B. E.; Jen, A. K.-Y.; Reid, P. J.; Dalton, L. R.; Robinson, B. H. Modeling the Optical Behavior of Complex Organic Media: From Molecules to Materials. *J. Phys. Chem. B* **2009**, *113*, 15581−15588.

(6) Firestone, K. A.; Lao, D. B.; Casmier, D. M.; Clot, O.; Dalton, L. R.; Reid, P. J. Frequency-Agile Hyper-Rayleigh Scattering Studies of Electro-Optic Chromophores. *Proc. SPIE* **2005**, *5395*, 0P1−0P9.

(7) Clays, K.; Persoons, A. Hyper-Rayleigh Scattering in Solution. *Rev. Sci. Instrum.* **1992**, *63*, 3285−3289.

(8) Oudar, J. L.; Chemla, D. S. Hyperpolarizabilities of the Nitroanilines and their Relations to the Excited State Dipole Moment. *J. Chem. Phys.* **1977**, *66*, 2664−2668.

(9) Cyvin, S. J.; Rauch, J. E.; Decius, J. C. Theory of Hyper-Raman Effects (Nonlinear Inelastic Light Scattering): Selection Rules and Depolarization Ratios for the Second-Order Polarizability. *J. Chem. Phys.* **1965**, *43*, 4083−4095.

(10) Castet, F.; Bogdan, E.; Plaquet, A.; Ducasse, L.; Champagne, B.; Rodriguez, V. Reference Molecules for Nonlinear Optics: a Joint Experimental and Theoretical Investigation. *J. Chem. Phys.* **2012**, *136*, No. 024506.

(11) Bale, D. H.; Eichinger, B. E.; Liang, W.; Li, X.; Dalton, L. R.; Robinson, B. H.; Reid, P. J. Dielectric Dependence of the First Molecular Hyperpolarizability for Electro-Optic Chromophores. *J. Phys. Chem. B* **2011**, *115*, 3505−3513.

(12) Rice, J. E.; Handy, N. C. The Calculation of Frequency-Dependent Polarizabilities as Pseudo-Energy Derivatives. *J. Chem. Phys.* **1991**, *94*, 4959−4971.

(13) Gerratt, J.; Mills, I. M. Force Constants and Dipole-Moment Derivatives of Molecules from Perturbed Hartree-Fock Calculations. I. *J. Chem. Phys.* **1968**, *49*, 1719−1729.

(14) Takimoto, Y.; Isborn, C. M.; Eichinger, B. E.; Rehr, J. J.; Robinson, B. H. Frequency and Solvent Dependence of Nonlinear Optical Properties of Molecules. *J. Phys. Chem. C* **2008**, *112*, 8016−8021.

(15) Meyers, F.; Marder, S. R.; Pierce, B. M.; Brédas, J. L. Electric Field Modulated Nonlinear Optical Properties of Donor- Acceptor Polyenes: Sum-Over-States Investigation of the Relationship between Molecular Polarizabilities (α,β, and γ) and Bond Length Alternation. *J. Am. Chem. Soc.* **1994**, *116*, 10703−10714.

(16) Kobayashi, R.; Koch, H.; Jørgensen, P. Calculation of Frequency-Dependent Polarizabilities Using Coupled-Cluster Response Theory. *Chem. Phys. Lett.* **1994**, *219*, 30−35.

(17) O'Neill, D. P.; Kallay, M.; Gauss, J. Calculation of Frequency-Dependent Hyperpolarizabilities using General Coupled-Cluster Models. *J. Chem. Phys.* **2007**, *127*, No. 134109.

(18) Suponitsky, K. Y.; Liao, Y.; Masunov, A. E. Electronic Hyperpolarizabilities for Donor-Acceptor Molecules with Long Conjugated Bridges: Calculations versus Experiment. *J. Phys. Chem. A* **2009**, *113*, 10994−11001.

(19) Hammond, J. R.; Kowalski, K. Parallel Computation of Coupled-Cluster Hyperpolarizabilities. *J. Chem. Phys.* **2009**, *130*, No. 194108.

(20) Davidson, E. R.; Eichinger, B. E.; Robinson, B. H. Hyperpolarizability: Calibration of theoretical methods for chloroform, water, acetonitrile, and p-nitroaniline. *Opt. Mater.* **2006**, *29*, 360−364.

(21) Suponitsky, K. Y.; Tafur, S.; Masunov, A. E. Applicability of Hybrid Density Functional Theory Methods to Calculation of Molecular Hyperpolarizability. *J. Chem. Phys.* **2008**, *129*, No. 044109.

(22) Castet, F.; Rodriguez, V.; Pozzo, J.-L.; Ducasse, L.; Plaquet, A.; Champagne, B. Design and Characterization of Molecular Nonlinear Optical Switches. *Acc. Chem. Res.* **2013**, *46*, 2656−2663.

(23) Reis, H. Problems in the Comparison of Theoretical and Experimental Hyperpolarizabilities Revisited. *J. Chem. Phys.* **2006**, *125*, No. 014506.

(24) Hohenberg, P. Inhomogeneous Electron Gas. *Phys. Rev.* **1964**, *136*, B864−B871.

(25) Kohn, W.; Sham, L. J. Self-Consistent Equations Including Exchange and Correlation Effects. *Phys. Rev.* **1965**, *140*, A1133−A1138.

(26) Pople, J. A.; Beveridge, D. L.; Dobosh, P. A. Approximate Self-Consistent Molecular-Orbital Theory. V. Intermediate Neglect of Differential Overlap. *J. Chem. Phys.* **1967**, *47*, 2026−2033.

(27) de Wergifosse, M.; Champagne, B. Electron Correlation Effects on the First Hyperpolarizability of Push-Pull pi-Conjugated Systems. *J. Chem. Phys.* **2011**, *134*, No. 074113.

(28) Jacquemin, D.; Champagne, B.; Hättig, C. Correlated Frequency-Dependent Electronic first Hyperpolarizability of Small Push−Pull Conjugated Chains. *Chem. Phys. Lett.* **2000**, *319*, 327−334.

(29) Christiansen, O.; Koch, H.; Jørgensen, P. The Second-Order Approximate Coupled Cluster Singles and Doubles Model CC2. *Chem. Phys. Lett.* **1995**, *243*, 409−418.

(30) Stephens, P. J.; Devlin, F. J.; Chabalowski, C. F.; Frisch, M. J. Ab Initio Calculation of Vibrational Absorption and Circular Dichroism Spectra Using Density Functional Force Fields. *J. Phys. Chem.* **1994**, *98*, 11623−11627.

(31) Becke, A. D. A New Mixing of Hartree-Fock and Local Density-Functional Theories. *J. Chem. Phys.* **1993**, *98*, 1372−1377.

(32) Andzelm, J.; Rinderspacher, B. C.; Rawlett, A.; Dougherty, J.; Baer, R.; Govind, N. Performance of DFT Methods in the Calculation of Optical Spectra of TCF-Chromophores. *J. Chem. Theory Comput.* **2009**, *5*, 2835−2846.

(33) Dreuw, A.; Head-Gordon, M. Single-Reference ab Initio Methods for the Calculation of Excited States of Large Molecules. *Chem. Rev.* **2005**, *105*, 4009−4037.

(34) Laurent, A. D.; Jacquemin, D. TD-DFT benchmarks: A Review. *Int. J. Quantum Chem.* **2013**, *113*, 2019−2039.

(35) Adamo, C.; Barone, V. Toward Reliable Density Functional Methods Without Adjustable Parameters: The PBE0Model. *J. Chem. Phys.* **1999**, *110*, 6158−6170.

(36) Jacquemin, D.; Perpéte, E. A.; Scuseria, G. E.; Ciofini, I.; Adamo, C. TD-DFT Performance for the Visible Absorption Spectra of Organic Dyes: Conventional versus Long-Range Hybrids. *J. Chem. Theory Comput.* **2008**, *4*, 123−135.

(37) Becke, A. D. Density-Functional Thermochemistry. III. The Role of Exact Exchange. *J. Chem. Phys.* **1993**, *98*, 5648−5652.

(38) Perdew, J. P.; Ernzerhof, M.; Burke, K. Rationale for Mixing Exact Exchange with Density Functional Approximations. *J. Chem. Phys.* **1996**, *105*, 9982−9985.

(39) Dreuw, A.; Head-Gordon, M. Failure of Time-Dependent Density Functional Theory for Long-Range Charge-Transfer Excited

States: The Zincbacteriochlorin−Bacteriochlorin and Bacteriochlorophyll−Spheroidene Complexes. *J. Am. Chem. Soc.* **2004**, *126*, 4007−4016.
(40) Magyar, R. J.; Tretiak, S. Dependence of Spurious Charge-Transfer Excited States on Orbital Exchange in TDDFT: Large Molecules and Clusters. *J. Chem. Theory Comput.* **2007**, *3*, 976−987.
(41) Lange, A.; Herbert, J. M. Simple Methods To Reduce Charge-Transfer Contamination in Time-Dependent Density-Functional Calculations of Clusters and Liquids. *J. Chem. Theory Comput.* **2007**, *3*, 1680−1690.
(42) Plötner, J.; Tozer, D. J.; Dreuw, A. Dependence of Excited State Potential Energy Surfaces on the Spatial Overlap of the Kohn-Sham Orbitals and the Amount of Nonlocal Hartree-Fock Exchange in Time-Dependent Density Functional Theory. *J. Chem. Theory Comput.* **2010**, *6*, 2315−2324.
(43) Champagne, B.; Perpéte, E. A.; Gisbergen, S. J. A. v.; Baerends, E.-J.; Snijders, J. G.; Soubra-Ghaoui, C.; Robins, K. A.; Kirtman, B. Assessment of Conventional Density Functional Schemes for Computing the Polarizabilities and Hyperpolarizabilities of Conjugated Oligomers: An ab initio Investigation of Polyacetylene Chains. *J. Chem. Phys.* **1998**, *109*, 10489−10498.
(44) Tawada, Y.; Tsuneda, T.; Yanagisawa, S.; Yanai, T.; Hirao, K. A Long-Range-Corrected Time-Dependent Density Functional Theory. *J. Chem. Phys.* **2004**, *120*, 8425−8433.
(45) Yanai, T.; Tew, D. P.; Handy, N. C. A New Hybrid Exchange−Correlation Functional Using the Coulomb-Attenuating method (CAM-B3LYP). *Chem. Phys. Lett.* **2004**, *393*, 51−57.
(46) Jacquemin, D.; Perpete, E. A.; Medved, M.; Scalmani, G.; Frisch, M. J.; Kobayashi, R.; Adamo, C. First Hyperpolarizability of Polymethineimine with Long-Range Corrected Functionals. *J. Chem. Phys.* **2007**, *126*, No. 191108.
(47) Foster, M. E.; Wong, B. M. Nonempirically Tuned Range-Separated DFT Accurately Predicts Both Fundamental and Excitation Gaps in DNA and RNA Nucleobases. *J. Chem. Theory Comput.* **2012**, *8*, 2682−2687.
(48) Srebro, M.; Autschbach, J. Tuned Range-Separated Time-Dependent Density Functional Theory Applied to Optical Rotation. *J. Chem. Theory Comput.* **2012**, *8*, 245−256.
(49) Sini, G.; Sears, J. S.; Brédas, J.-L. Evaluating the Performance of DFT Functionals in Assessing the Interaction Energy and Ground-State Charge Transfer of Donor/Acceptor Complexes: Tetrathiafulvalene−Tetracyanoquinodimethane (TTF−TCNQ) as a Model Case. *J. Chem. Theory Comput.* **2011**, *7*, 602−609.
(50) Tao, J.; Perdew, J.; Staroverov, V.; Scuseria, G. Climbing the Density Functional Ladder: Nonempirical Meta−Generalized Gradient Approximation Designed for Molecules and Solids. *Phys. Rev. Lett.* **2003**, *91*, No. 146401.
(51) Tao, J.; Perdew, J. Nonempirical Construction of Current-Density Functionals from Conventional Density-Functional Approximations. *Phys. Rev. Lett.* **2005**, *95*, No. 196403.
(52) Schwabe, T.; Grimme, S. Towards Chemical Accuracy for the Thermodynamics of Large Molecules: New Hybrid Density Functionals Including Non-Local Correlation Effects. *Phys. Chem. Chem. Phys.* **2006**, *8*, 4398−4401.
(53) Zhao, Y.; Schultz, N. E.; Truhlar, D. G. Design of Density Functionals by Combining the Method of Constraint Satisfaction with Parametrization for Thermochemistry, Thermochemical Kinetics, and Noncovalent Interactions. *J. Chem. Theory Comput.* **2006**, *2*, 364−382.
(54) Zhao, Y.; Truhlar, D. G. Density Functionals with Broad Applicability in Chemistry. *Acc. Chem. Res.* **2008**, *41*, 157−167.
(55) Zerner, M. An Approximate Molecular Orbital Method. *J. Chem. Phys.* **1975**, *62*, 2788−2799.
(56) Caricato, M.; Mennucci, B.; Tomasi, J. Solvent Effects on the Electronic Spectra: An Extension of the Polarizable Continuum Model to the ZINDO Method. *J. Phys. Chem. A* **2004**, *108*, 6248−6256.
(57) Gaussian 09 User's Reference. Gaussian, Inc.: Wallingford, CT, 2011. http://www.gaussian.com/g_tech/g_ur/k_dft.htm (accessed 03/26/2012).
(58) Zhao, Y.; Truhlar, D. G. The M06 Suite of Density Functionals for Main Group Thermochemistry, Thermochemical Kinetics, Noncovalent Interactions, Excited States, and Transition Elements: Two New Functionals and Systematic Testing of Four M06-Class Functionals and 12 Other Functionals. *Theor. Chem. Acc.* **2007**, *120*, 215−241.
(59) Chai, J. D.; Head-Gordon, M. Systematic Optimization of Long-Range Corrected Hybrid Density Functionals. *J. Chem. Phys.* **2008**, *128*, No. 084106.
(60) Peverati, R.; Truhlar, D. G. Improving the Accuracy of Hybrid Meta-GGA Density Functionals by Range Separation. *J. Phys. Chem. Lett.* **2011**, *2*, 2810−2817.
(61) Stewart, J. J. Optimization of Parameters for Semiempirical Methods V: Modification of NDDO Approximations and Application to 70 Elements. *J. Mol. Model.* **2007**, *13*, 1173−1213.
(62) Firestone, K. A. Frequency-agile hyper-Rayleigh scattering studies of nonlinear optical chromophores. Ph.D. Thesis, University of Washington, Seattle, 2005.
(63) Frisch, M. J.; Trucks, G. W.; Schlegel, H. B.; Scuseria, G. E.; Robb, M. A.; Cheeseman, J. R.; Scalmani, G.; Barone, V.; Mennucci, B.; Petersson, G. A.; Nakatsuji, H.; Caricato, M.; Li, X.; Hratchian, H. P.; Izmaylov, A. F.; Bloino, J.; Zheng, G.; Sonnenberg, J. L.; Hada, M.; Ehara, M.; Toyota, K.; Fukuda, R.; Hasegawa, J.; Ishida, M.; Nakajima, T.; Honda, Y.; Kitao, O.; Nakai, H.; Vreven, T.; Montgomery, J. A., Jr.; Peralta, J. E.; Ogliaro, F.; Bearpark, M.; Heyd, J. J.; Brothers, E.; Kudin, K. N.; Staroverov, V. N.; Kobayashi, R.; Normand, J.; Raghavachari, K.; Rendell, A.; Burant, J. C.; Iyengar, S. S.; Tomasi, J.; Cossi, M.; Rega, N.; Millam, J. M.; Klene, M.; Knox, J. E.; Cross, J. B.; Bakken, V.; Adamo, C.; Jaramillo, J.; Gomperts, R.; Stratmann, R. E.; Yazyev, O.; Austin, A. J.; Cammi, R.; Pomelli, C.; Ochterski, J. W.; Martin, R. L.; Morokuma, K.; Zakrzewski, V. G.; Voth, G. A.; Salvador, P.; Dannenberg, J. J.; Dapprich, S.; Daniels, A. D.; Farkas, O.; Foresman, J. B.; Ortiz, J. V.; Cioslowski, J.; Fox, D. J. *Gaussian 09*, revision C.01; Gaussian, Inc.: Wallingford, CT, 2009.
(64) Szabo, A.; Ostlund, N. S. *Modern Quantum Chemistry: Introduction to Advanced Electronic Structure Theory*, 1st (revised) ed.; Dover Publications, Inc.: New York, NY, 1989.
(65) Risko, C.; McGehee, M. D.; Brédas, J.-L. A Quantum-Chemical Perspective into Low Optical-Gap Polymers for Highly-Efficient Organic Solar Cells. *Chem. Sci.* **2011**, *2*, 1200−1218.
(66) Korzdorfer, T.; Sears, J. S.; Sutton, C.; Bredas, J. L. Long-Range Corrected Hybrid Functionals for pi-Conjugated Systems: Dependence of the Range-Separation Parameter on Conjugation Length. *J. Chem. Phys.* **2011**, *135*, No. 204107.
(67) Champagne, B.; Bulat, F. A.; Yang, W.; Bonness, S.; Kirtman, B. Density functional theory investigation of the polarizability and second hyperpolarizability of polydiacetylene and polybutatriene chains: Treatment of exact exchange and role of correlation. *J. Chem. Phys.* **2006**, *125*, No. 194114.
(68) Borini, S.; Limacher, P. A.; Luthi, H. P. A Systematic Analysis of the Structure and (Hyper)polarizability of Donor-Acceptor Substituted Polyacetylenes using a Coulomb-Attenuating Density Functional. *J. Chem. Phys.* **2009**, *131*, No. 124105.
(69) Torrent-Sucarrat, M.; Anglada, J. M.; Luis, J. M. Evaluation of the Nonlinear Optical Properties for Annulenes with Hückel and Möbius Topologies. *J. Chem. Theory Comput.* **2011**, *7*, 3935−3943.
(70) Lu, S. I. Computational Study of Static First Hyperpolarizability of Donor-Acceptor Substituted (E)-Benzaldehyde Phenylhydrazone. *J. Comput. Chem.* **2011**, *32*, 730−736.
(71) Johnson, L. E. Multi-Scale Modeling of Organic Electro-Optic Materials. University of Washington, Seattle, 2012.